RELAXATION OSCILLATORS AND NETWORKS

Relaxation oscillations comprise a large class of nonlinear dynamical systems, and arise naturally from many physical systems such as mechanics, geology, biology, chemistry, and engineering. Such periodic phenomena are characterized by intervals of time during which little happens, interleaved with intervals of time during which considerable changes take place. In other words, relaxation oscillations exhibit two time scales. The dynamics of a relaxation oscillator is illustrated by the mechanical system of a seesaw in Figure 1. At one side of the seesaw is there a water container which is empty at the beginning; in this situation the other side of the seesaw touches the ground. As the weight of water running from a tap into the container exceeds that of the other side, the seesaw flips and the container side touches the ground. At this moment, the container empties itself, and the seesaw returns quickly to its original position and the process repeats.

Relaxation oscillations were first observed by van der Pol [1] in 1926 when studying properties of a triode circuit. Such a circuit exhibits self-sustained oscillations. van der Pol discovered that for a certain range of system parameters the oscillation is almost sinusoidal, but for a different range the oscillation exhibits abrupt changes. In the latter case, the period of the oscillation is proportional to the relaxation time (time constant) of the system, hence the term *relaxation oscillation*. van der Pol [2] later gave the following defining properties of relaxation oscillations:

1. The period of oscillations is determined by some form of relaxation time.
2. They represent a periodic autonomous repetition of a typical aperiodic phenomenon.
3. Drastically different from sinusoidal or harmonic oscillations, relaxation oscillators exhibit discontinuous jumps.
4. A nonlinear system with implicit threshold values, characteristic of the all-or-none law.

A variety of biological phenomena can be characterized as relaxation oscillations, ranging from heartbeat, neuronal activity, to population cycles; the English physiologist Hill [3] even went as far as saying that relaxation oscillations are the type of oscillations that governs all periodic phenomena in physiology.

Given that relaxation oscillations have been studied in a wide range of domains, it would be unrealistic to provide an up-to-date review of all aspects in this article. Thus, I choose to orient my description towards neurobiology and emphasize networks of relaxation oscillators based on the following two considerations (the reader is referred to [4] for an extensive coverage of relaxation oscillations). First, as described in the next section, neurobiology has motivated a great deal of study on relaxation oscillations. Second, substantial progress has been made in understanding networks of relaxation oscillators. In the next section, I describe a number of relaxation oscillators, including the van der Pol oscillator. The following section is devoted to networks of relaxation oscillators, where the emergent phenomena of synchrony and desynchrony are the major topics. Then, I describe applications of relaxation oscillator networks to visual and auditory scene analysis, which are followed by some concluding remarks.

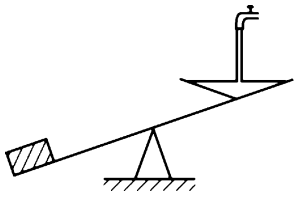

Figure 1. An example of a relaxation oscillator: a seesaw with a water container at one end (adapted from [4]).

RELAXATION OSCILLATORS

In this section I introduce four relaxation oscillators. The van der Pol oscillator exemplifies relaxation oscillations, and has played an important role in the development of dynamical systems, in particular nonlinear oscillations. The Fitzhugh-Nagumo oscillator and the Morris-Lecar oscillator are well-known models for the conductance-based membrane potential of a nerve cell. The Terman-Wang oscillator has underlain a number of studies on oscillator networks and their applications to scene analysis. As demonstrated by Nagumo et al. [5] and Keener [6], these oscillator models can be readily implemented with electrical circuits.

Van der Pol Oscillator

The van der Pol oscillator can be written in the form

$$\ddot{x} + x = c(1 - x^2)\dot{x} \tag{1}$$

where $c > 0$ is a parameter. This second-order differential equation can be converted to a two variable first-order differential equation,

$$\dot{x} = c[y - f(x)] \tag{2}$$

$$\dot{y} = -x/c \tag{2}$$

Here $f(x) = -x + x^3/3$. The x nullcline, i.e. $\dot{x} = 0$, is a cubic curve, while the y nullcline, $\dot{y} = 0$, is the y axis. As shown in Fig. 2(a), the two nullclines intersect along the middle branch of the cubic, and the resulting fixed point is unstable as indicated by the flow field in the phase plane of Fig. 2(a). This equation yields a periodic solution.

As $c > 1$, Eq. (2) yields two time scales: a slow time scale for they variable and a fast time scale for the x variable. As a result, Eq. (2) becomes the van der Pol oscillator that produces a relaxation oscillation. The limit cycle for the van der Pol oscillator is given in Fig. 2(b), and it is composed of four pieces, two slow ones indicated by pq and rs, and two fast ones indicated by qr and sp. In other words, motion along the two branches of the cubic is slow compared to fast alternations, or jumps, between the two branches. Fig. 2(c) shows x activity of the oscillator with respect to time, where two time scales are clearly indicated by relatively slow changes in x activity interleaving with fast changes.

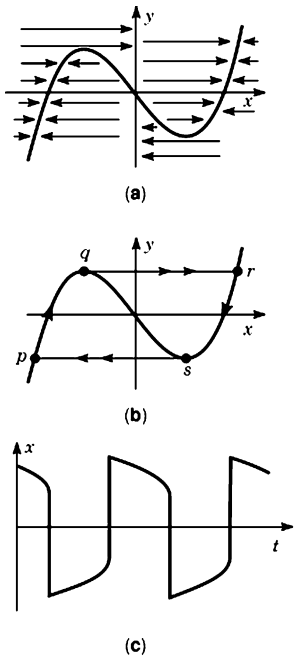

Figure 2. Phase portrait and trajectory of a van der Pol oscillator. (a) Phase portrait. The x nullcline is the cubic curve, and the y nullcline is the y axis. Arrows indicate phase flows. (b) limit cycle orbit. The limit cycle is labeled as $pqrs$, and the arrowheads indicate the direction of motion. Within the limit cycle, qr and sp are two fast pieces (indicated by double arrowheads), and pq and rs are slow pieces. (c) Temporal activity of the oscillator. Here the x activity is shown with respect to time.

FitzHugh-Nagumo Oscillator

By simplifying the classical Hodgkin-Huxley equations [5] for modeling nerve membranes and action potential generation, FitzHugh [7] and Nagumo et al. [8] gave the following two-variable equation, widely known as the FitzHugh-Nagumo model,

$$\dot{x} = c[y - f(x) + I] \tag{3}$$

$$\dot{y} = -(x + by - a)/c \tag{3}$$

where $f(x)$ is as defined in Eq. (2), I is the injected current, and a, b, and c are system parameters satisfying the conditions: $1 > b > 0$, $c^2 > b$, and $1 > a > 1 - 2b/3$. In neurophysiological terms, x corresponds to the neuronal membrane potential, and y plays the aggregate role of three variables in the Hodgkin-Huxley equations. Given that the x nullcline is a cubic and the y nullcline is linear, the FitzHugh-Nagumo equation is mathematically similar to the van der Pol equation. Typical relaxation oscillation with two time scales occurs when $c > 1$. Because of the three parameters and the external input I, the FitzHugh-Nagumo oscillator has additional flexibility. Depending on parameter values, the oscillator can exhibit a stable steady state or a stable periodic orbit. With a perturbation by external stimulation, the steady state can become unstable and be replaced by an oscillation; the steady state is thus referred to as the *excitable* state.

Morris-Lecar Oscillator

In modeling voltage oscillations in barnacle muscle fibers, Morris and Lecar [9] proposed the following equation,

$$\dot{x} = -g_{Ca} m_\infty(x)(x - 1) - g_K y(x - x_K) - g_L(x - x_L) + I \tag{4}$$

$$\dot{y} = -\varepsilon[y_\infty(x) - y]/\tau_y(x) \tag{4}$$

where

$$\begin{aligned} m_\infty(x) &= \{1 + \tanh[(x - x_1)/x_2]\}/2 \\ y_\infty(x) &= \{1 + \tanh[(x - x_3)/x_4]\}/2 \\ \tau_y(x) &= 1/\cosh[(x - x_3)/(2x_4)] \end{aligned}$$

and x_1 x_2, x_3, x_4, g_{Ca}, g_K, g_L, x_K, and x_L are parameters. Ca stands for calcium, K for potassium, L for leak, and I is the injected current. The parameter ε controls relative time scales of x and y. Like Eq. (3), the Morris-Lecar oscillator is closely related to the Hodgkin-Huxley equations, and it is used as a two-variable description of neuronal membrane properties or the envelope of an oscillating burst [10]. The x variable corresponds to the membrane potential, and y corresponds to the state of activation of ionic channels.

The x nullcline of Eq. (4) resembles a cubic and the y nullcline is a sigmoid. When ε is chosen to be small, the Morris-Lecar equation produces typical relaxation oscillations. From the mathematical point of view, the sigmoidal y nullcline marks the major difference between the Morris-Lecar oscillator and the FitzHugh-Nagumo oscillator.

Terman-Wang Oscillator

Motivated by mathematical and computational considerations, Terman and Wang [11] proposed the following equation,

$$\dot{x} = f(x) - y + I \tag{5}$$

$$\dot{y} = \varepsilon[g(x) - y] \tag{5}$$

where $f(x) = 3x - x^3 + 2$, $g(x) = \alpha[1 + \tanh(x/\beta)]$, and I represents external stimulation to the oscillator. Thus x nullcline is a cubic and the y nullcline is a sigmoid, where α and β are parameters. When $\varepsilon \ll 1$, Eq. (5) defines a typical relaxation oscillator. When $I > 0$ and with a small β, the two nullclines intersect only at a point along the middle branch of the cubic and the oscillator produces a stable periodic orbit (see Fig. 3(a)). The periodic solution alternates between *silent* (low x) and *active* (high x) phases of near steady-state behavior. As shown in Fig. 3(a), the silent and the active phases correspond to the left branch (LB) and the right branch (RB) of the cubic, respectively. If $I < 0$, the two nullclines of Eq. (5) intersect at a stable fixed point along the left branch of the cubic (see Fig. 3(b)), and the oscillator is in the excitable state. The parameter α determines relative times that the periodic solution spends in these two phases. A larger α results in a relatively shorter active phase.

The Terman-Wang oscillator is similar to the aforementioned oscillator models. It is much simpler than the Morris-Lecar oscillator, and provides a dimension of flexibility absent in the van der Pol and FitzHugh-Nagumo equations. In neuronal terms, the x variable in Eq. (5) cor-

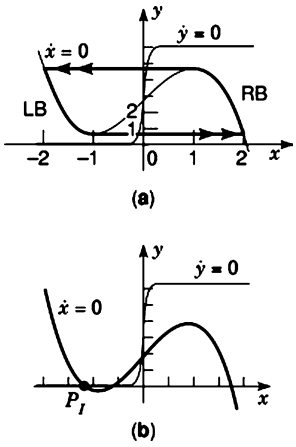

Figure 3. Nullclines and trajectories of a Terman-Wang oscillator. (a) Behavior of a stimulated oscillator. The x nullcline is a cubic and the y nullcline is a sigmoid. The limit cycle is shown with a bold curve, and its direction of motion is indicated by arrowheads. LB and RB denote the left branch and the right branch of the cubic, respectively, (b) Behavior of an excitable (unstimulated) oscillator. The oscillator approaches the stable fixed point P_I.

responds to the membrane potential, and y the state for channel activation or inactivation.

NETWORKS OF RELAXATION OSCILLATORS

In late eighties, neural oscillations in the gamma frequency range (about 40 Hz) were discovered to in the visual cortex [12] [13]. The experimental findings can be summarized as the following: (1) neural oscillations are triggered by sensory stimulation, and thus the oscillations are stimulus-dependent; (2) long-range synchrony with zero phase-lag occurs if the stimuli appear to form a coherent object; (3) no synchronization occurs if the stimuli appear to be unrelated. These intriguing observations are consistent with the *temporal correlation* theory [14], which states that in perceiving a coherent object the brain links various feature detecting neurons via temporal correlation among the firing activities of these neurons.

Since the discovery of coherent oscillations in the visual cortex and other brain areas, neural oscillations and synchronization of oscillator networks have been extensively studied. Most of the early models are based on sinusoidal or harmonic oscillators and rely on all-to-all connectivity to reach synchronization across the network. In fact, according to the Mermin and Wagner theorem [15] in statistical physics, no synchrony exists in one- or two-dimensional locally coupled isotropic Heisenberg oscillators, which are similar to harmonic oscillators. However, all-to-all connectivity leads to indiscriminate synchrony because the network is dimensionless and loses critical information about topology. Thus, such networks are very limited in addressing perceptual organization and scene analysis – the main motivations behind computational studies of oscillatory networks – that appear to require topological relations.

Somers and Kopell [16] and Wang [17] first realized that there are qualitative differences between sinusoidal and non-sinusoidal oscillators in achieving emergent synchrony in a locally coupled network. Specifically, Somers and Kopell using relaxation oscillators and Wang using Wilson-Cowan oscillators [18] each demonstrated that an oscillator network can synchronize with just local coupling. Note that Wilson-Cowan oscillators in their normal parameter regime are neither sinusoidal nor relaxation-type.

Two Oscillators: Fast Threshold Modulation

When analyzing synchronization properties of a pair of relaxation oscillators, Somers and Kopell [16] introduced the notion *of fast threshold modulation*. Their mechanism works for general relaxation oscillators, including those described in the previous section. Consider a pair of identical relaxation oscillators excitatorily coupled in a way mimicking chemical synapses. The coupling is between the fast variables of the two oscillators, and can be viewed as binary, resulting in the so-called Heaviside coupling. The two oscillators are uncoupled unless one of them is in the active phase, and in this case the effect of the excitatory coupling is to raise the cubic of the other oscillator by a fixed amount.

Let us explain the mechanism of fast threshold modulation using the Terman-Wang oscillator as an example. The two oscillators are denoted by $o_1 = (x_1,\ y_1)$ and $o_2 = (x_2,\ y_2)$, which are initially in the silent phase and close to each other with o_1 leading the way as illustrated in Fig. 4. Figure 4 shows the solution of the oscillator system in the singular limit $\varepsilon \to 0$. The singular solution consists of several pieces. The first piece is when both oscillators move along LB of the uncoupled cubic, denoted as C. This piece lasts until o_1 reaches the left knee of C, LK, at $t = t_1$. The second piece begins when o_1 jumps up to RB, and the excitatory coupling from o_1 to o_2 raises the cubic for o_2 from C to C_E as shown in the figure. Let LK_E and RK_E denote the left and right knees of C_E. If $|y_1 - y_2|$ is relatively small, then o_2 lies below LK_E and jumps up. Since these interactions take place in fast time, the oscillators are effectively synchronized in jumping up. As a result the cubic for o_1 is raised to C_E as well. The third piece is when both oscillators lie on RB and evolve in slow time. Note that the ordering in which the two oscillators track along RB is reversed and now o_2 leads the way. The third piece lasts until o_2 reaches RK_E at $t = t_2$. The fourth piece starts when o_2 jumps down to LB. With o_2 jumping down, the cubic for o_1 is lowered to C. At this time, if o_1 lies above RK, as shown in Fig. 4, o_1 jumps down as well and both oscillators are now in the silent phase. Once both oscillators are on LB, the above analysis repeats.

Based on the fast threshold modulation mechanism, Somers and Kopell further proved a theorem that the synchronous solution in the oscillator pair has a domain of attraction in which the approach to synchrony has a geometric (or exponential) rate [16]. The Somers-Kopell theorem is based on comparing the evolution rates of the slow variable right before and after a jump, which are determined by the vertical distance of an oscillator to they nullcline (see Fig. 4).

A Network of Locally Coupled Oscillators

In the same paper Somers and Kopell suspected that their analysis extends to a network of relaxation oscillators, and

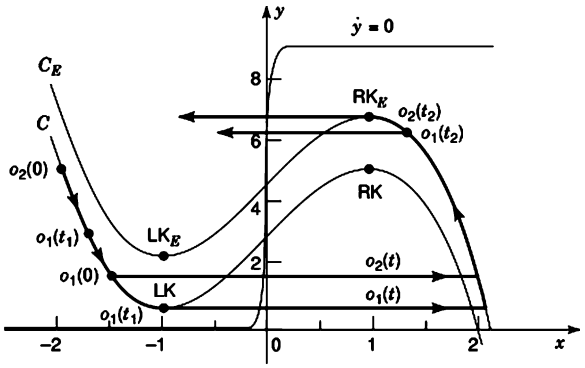

Figure 4. Fast threshold modulation. C and C_E indicate the uncoupled and the excited cubic, respectively. The two oscillators o_1 and o_2 start at time 0. When o_1 jumps up at $t = t_1$, the cubic corresponding to o_2 is raised from C to C_E. This allows o_2 to jump up as well. When o_2 jumps down at $t = t_2$, the cubic corresponding to o_1 is lowered from C_E to C. This allows o_1 to jump down as well. In the figure, LK and RK indicate the left knee and the right knee of C, respectively. LK_E and RK_E indicate the left knee and right knee of C_E, respectively.

performed numerical simulations with one-dimensional rings to support their suggestion. In a subsequent study, by extending Somers and Kopell analysis, Terman and Wang proved a theorem that for an arbitrary network of locally coupled relaxation oscillators there is a domain of attraction in which the entire network synchronizes at an exponential rate [11].

In their analysis, Terman and Wang employed the time metric to describe the distance between oscillators. When oscillators evolve either in the silent phase or the active phase, their distances in y in the Euclidean metric change; however, their distances in the time metric remain constant. On the other hand, when oscillators jump at the same time (in slow time), their y distances remain unchanged while their time distances change. Terman and Wang also introduced the condition that the sigmoid for the y nullcline (again consider the Terman-Wang oscillator) is very close to a step function [11], which is the case when β in Eq. (5) is chosen to be very small. This condition implies that in the situation with multiple cubics the rate of evolution of a slow variable does not depend on which cubic it tracks along.

Recently, Campbell et al. [19] showed that the definition of a canonical relaxation oscillator can lead to qualitatively different kinds of oscillation through parameter choices. In addition, their numerical investigation indicates that a network of relaxation oscillators in the relaxation regime (the normal case) approach synchrony with an average time that is a power relation of the network size with a small exponent. On the other hand, relaxation oscillators in the spiking regime, where the active phase is much shorter than the silent phase, approach synchrony with an average time that is a logarithmic relation of the network size, although for the same network synchrony in the relaxation regime is typically faster than that in the spiking relation.

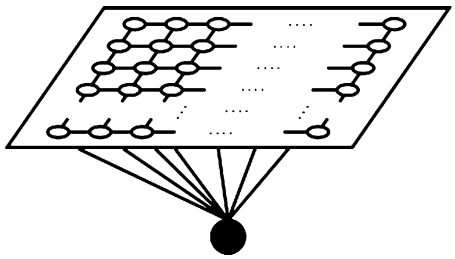

Figure 5. Architecture of a two dimensional LEGION network with nearest neighbor coupling. The global inhibitor is indicated by the black circle, and it receives excitation from every oscillator of the 2-D grid and feeds back inhibition to every oscillator.

LEGION Networks: Selective Gating

A natural and special form of the temporal correlation theory is *oscillatory correlation* [20], whereby each object is represented by synchronization of the oscillator group corresponding to the object and different objects in a scene are represented by different oscillator groups which are desynchronized from each other. There are two fundamental aspects in the oscillatory correlation theory: synchronization and desynchronization. Extending their results on synchronizing locally coupled relaxation oscillators, Terman and Wang used a global inhibitory mechanism to achieve desynchronization [11]. The resulting network is called LEGION, standing for Locally Excitatory Globally Inhibitory Oscillator Networks [20].

The original description of LEGION is based on Terman-Wang oscillators, and basic mechanisms extend to other relaxation oscillator models. Each oscillator i is defined as

$$\dot{x}_i = f(x_i) - y_i + I_i + S_i + \rho \tag{6}$$

$$\dot{y}_i = \varepsilon[g(x_i) - y_i] \tag{6}$$

Here $f(x)$ and $g(x)$ are as given in Eq. (5). The parameter ρ denotes the amplitude of Gaussian noise; to reduce the chance of self-generating oscillations the mean of noise is set to $-\rho$. In addition to test robustness, noise plays the role of assisting desynchronization. The term S_i denotes the overall input from other oscillators in the network:

$$S_i = \sum_{k \in N(i)} W_{ik} H(x_k - \theta_x) - W_z H(z - \theta_z) \tag{7}$$

where W_{ik} is the *dynamic* connection weight from k to i, and $N(i)$ is the set of the adjacent oscillators that connect to i. In a two-dimensional (2-D) LEGION network, $N(i)$ in the simplest case contains four immediate neighbors except on boundaries where no wrap-around is used, thus forming a 2-D grid. This architecture is shown in Fig. 5. H stands for the Heaviside function, defined as $H(\nu) = 1$ and $H(\nu) = 0$ if $\nu < 0$. θ_x is a threshold above which an oscillator can affect its neighbors. W_z is the weight of inhibition from the global inhibitor z, whose activity is defined as

$$\dot{z} = \phi(\sigma_\infty - z) \tag{8}$$

where ϕ is a parameter. The quantity $\sigma_\infty = 1$ if $x_i \geq \theta_z$ for at least one oscillator i, and $\sigma_\infty = 0$ otherwise. Hence θ_z (see also Eq. (7)) represents a threshold.

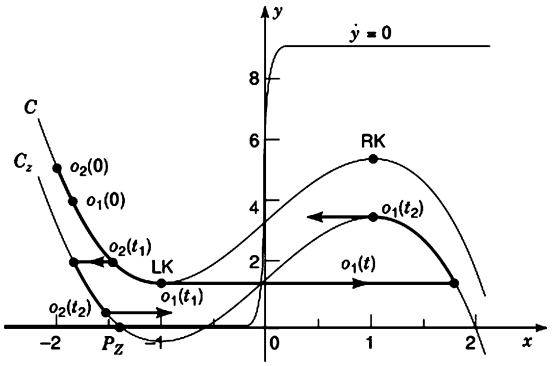

Figure 6. Selective gating with two oscillators coupled through a global inhibitor. C and C_Z indicate the uncoupled and the inhibited cubic, respectively. The two oscillators o_1 and o_2 start at time 0. When o_1 jumps up at $t = t_1$ the cubic corresponding to both o_1 and o_2 is lowered from C to C_Z. This prevents o_2 from jumping up until o_1 jumps down at $t = t_2$ and releases o_2 from the inhibition. LK and RK indicate the left knee and the right knee of C, respectively. P_Z denotes a stable fixed point at an intersection point between C_Z and the sigmoid.

The dynamic weights W_{ik}'s are formed on the basis of permanent weights T_{ik}'s according to the mechanism of dynamic normalization [21] [22], which ensures that each oscillator has equal overall weights of dynamic connections, W_T, from its neighborhood. According to Ref. [11], weight normalization is not a necessary condition for LEGION to work, but it improves the quality of synchronization. Moreover, based on external input W_{ik} can be determined at the start of simulation.

To illustrate how desynchronization between blocks of oscillators is achieved in a LEGION network, let us consider an example with two oscillators that are coupled only through the global inhibitor. Each oscillator is meant to correspond to an oscillator block that represents a pattern in a scene. The same notations introduced earlier are used here. Again, assume that both oscillators are in the silent phase and close to each other with $y_1 < y_2$, as shown in Fig. 6. The singular solution of the system consists of several pieces, where the first one lasts until o_1 reaches LK at $t = t_1$. When both oscillators are on LB, $z = 0$. The second piece starts when o_1 jumps up, and when o_1 crosses θ_z, σ_∞ switches from 0 to 1, and $z \to 1$ on the fast time scale. When z crosses θ_z, the cubic corresponding to both o_1 and o_2 lowers from C to C_Z, the inhibited cubic. The third piece is when o_1 is the active phase, while o_2 is in the silent phase. The parameters are chosen so that C_Z intersects with the sigmoid at a stable fixed point P_Z along LB as shown in Fig. 6. This guarantees that $o_2 \to P_Z$, and o_2 cannot jump up as long as o_1 is on RB, which lasts until o_1 reach the right knee of C_Z at $t = t_2$. The fourth piece starts when o_1 jumps down to LB. When o_1 crosses θ_z, $z \to 0$ in fast time. When z crosses θ_z, the cubic corresponding to both o_1 and o_2 returns to C. There are now two cases to consider. If o_2 lies below LK, as shown in Fig. 6, then o_2 jumps up immediately. Otherwise both o_1 and o_2 lie on LB, with o_2 leading the way. This new silent phase terminates when o_2 reaches LK and jumps up.

The above analysis demonstrates the role of inhibition in desynchronizing the two oscillators: o_1 and o_2 are never in the active phase simultaneously. In general, LEGION exhibits a mechanism of *selective gating*, whereby an oscillator, say o_i jumping to its active phase quickly activates the global inhibitor, which selectively prevents the oscillators representing different blocks from jumping up, without affecting o_i's ability in recruiting the oscillators of the same block because of local excitation. With the selective gating mechanism, Terman and Wang proved the following theorem. For a LEGION network there is a domain of parameters and initial conditions in which the network achieves both synchronization within blocks of oscillators and desynchronization between different blocks in no greater than N cycles of oscillations, where N is the number of patterns in an input scene. In other words, both synchronization and desynchronization are achieved rapidly.

The following simulation illustrates the process of synchronization and desynchronization in LEGION [20]. Four patterns – two **O**'s, one **H**, and one **I**, forming the word **OHIO** – are simultaneously presented to a 20 × 20 LEGION network as shown in Figure 7(a). Each pattern is a connected region, but no two patterns are connected to each other. The oscillators under stimulation become oscillatory, while those without stimulation remain excitable. The parameter ρ is set to represent 10% noise compared to the external input. The phases of all the oscillators on the grid are randomly initialized. Figs. 7(b)–7(f) show the instantaneous activity (snapshot) of the network at various stages of dynamic evolution. Fig. 7(b) shows a snapshot of the network at the beginning of the simulation, displaying the random initial conditions. Fig. 7(c) shows a snapshot shortly afterwards. One can clearly see the effect of synchronization and desynchronization: all the oscillators corresponding to the left **O** are entrained and have large activity; at the same time, the oscillators stimulated by the other three patterns have very small activity. Thus the left **O** is segmented from the rest of the input. Figures 7(d)–(f) show subsequent snapshots of the network, where different patterns reach the active phase and segment from the rest. This successive "popout" of the objects continues in an approximately periodic fashion as long as the input stays on. To provide a complete picture of dynamic evolution, Fig. 7(g) shows the temporal evolution of every oscillator. Synchronization within each object and desynchronization between them are clearly shown in three oscillation periods, which is consistent with the theorem proven in [11].

Time Delay Networks

Time delays in signal transmission are inevitable in both the brain and physical systems. In local cortical circuits, for instance, the speed of nerve conduction is less than 1 mm/ms such that connected neurons 1 mm apart have a time delay of more than 4% of the period of oscillation assuming 40 Hz oscillations. Since small delays may completely alter the dynamics of differential equations, it is important to understand how time delays change the behavior, particularly synchronization, of relaxation oscillator networks.

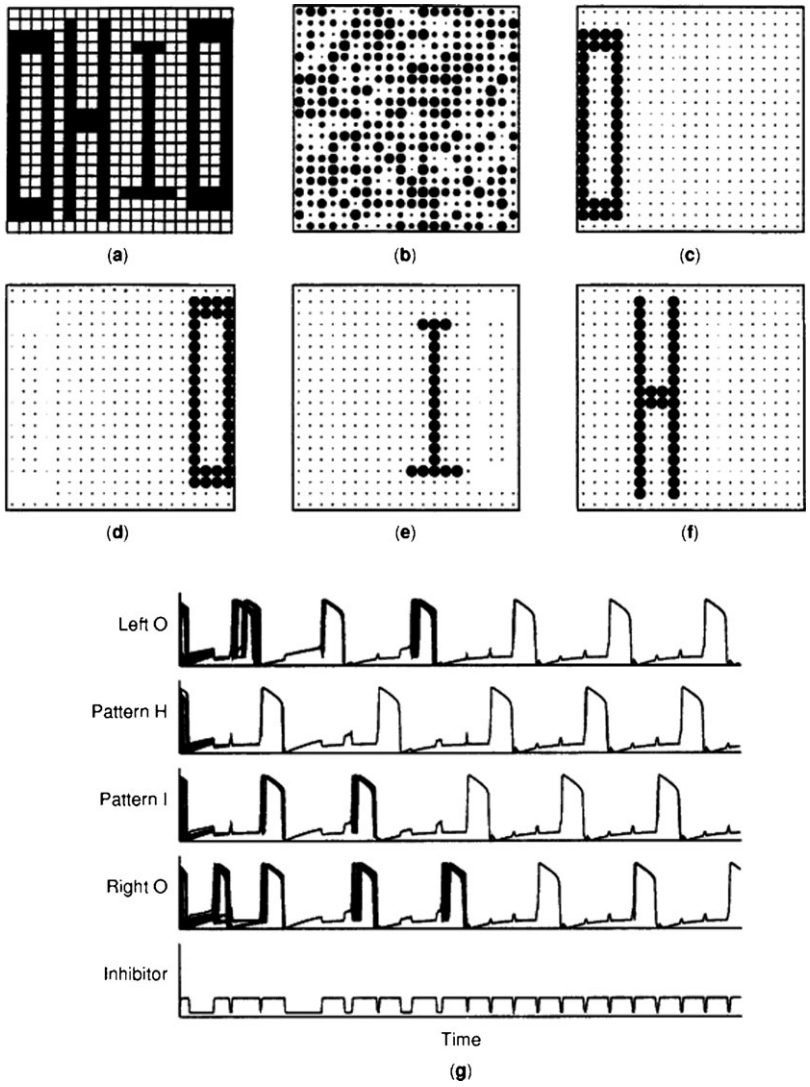

Figure 7. Synchronization and desynchronization in LEGION. (a) A scene composed of four patterns which were presented (mapped) to a 20 × 20 LEGION network. (b) A snapshot of the activities of the oscillator grid at the beginning of dynamic evolution. The diameter of each black circle represents the x activity of the corresponding oscillator. (c) A snapshot taken shortly after the beginning. (d) Another snapshot taken shortly after (c). (e) Another snapshot taken shortly after (d). (f) Another snapshot taken shortly after (e). (g) The upper four traces show the combined temporal activities of the oscillator blocks representing the four patterns, respectively, and the bottom trace shows the temporal activity of the global inhibitor. The ordinate indicates the normalized x activity of an oscillator. Since the oscillators receiving no external input are excitable during the entire simulation process, they are excluded from the display. The activity of the oscillators stimulated by each object is combined into a single trace in the figure. The differential equations were solved using a fourth-order Runge-Kutta method (from [20]).

Campbell and Wang [23] studied locally coupled relaxation oscillators with time delays. They revealed the phenomenon of loose synchrony in such networks. Loose synchrony in networks with nearest neighbor coupling is defined as follows. Coupled oscillators approach each other so that their time difference is less than or equal to the time delay between them. They analyzed a pair of oscillators in the singular limit $\varepsilon \to 0$, and gave a precise diagram in parameter space that indicates regions of distinct dynamical behavior, including loosely synchronous and antiphase solutions. The diagram points out that loose synchrony exists for a wide range of time delays and initial conditions. Numerical simulations show that the singular solutions derived by them extend to the case $0 < \varepsilon \ll 1$. Furthermore, through extensive simulations they conclude that their parameter diagram for a pair of oscillators says much about networks of locally coupled relaxation oscillators. In particular, the phenomenon of loose synchrony exists in a similar way. Figure 8 demonstrates loosely synchronous behavior in a chain of 50 oscillators with a time delay that is 3% of the oscillation period between adjacent oscillators. The phase relations between the oscillators in the chain become stabilized by the third cycle.

Two other results regarding relaxation oscillator networks with time delays are worth mentioning. First, Campbell and Wang [23] identified a range of initial conditions in which the maximum time delays between any two oscillators in a locally coupled network can be contained. Second, they found that in LEGION networks with time delay coupling between oscillators, desynchronous solutions for different oscillator blocks are maintained. Thus, the introduction of time delays does not appear to impact the behavior of LEGION in terms of synchrony and desynchrony.

Subsequently, Fox et al. [24] proposed a method to achieve zero phase-lag synchrony in locally coupled relaxation oscillators with coupling delays. They observed that different speeds of motion along different nullclines could result in rapid synchronization. Their analysis in particular shows how to choose appropriate y nullclines to induce different speeds of motion, which in turn lead to zero-lag synchrony. Numerical simulations demonstrate that their analytical results obtained in the case of two coupled oscillators extend to 1-D and 2-D networks. More recently, Sen and Rand [25] numerically investigated the dynam-

ics of a pair of van der Pol oscillators coupled with time delays. Their comprehensive analysis revealed regions in the 2-D plane of coupling strength and time delay where stable zero-lag synchrony occurs, as well as regions where antiphase solutions exist. Interestingly, there is an overlap between synchronous and antiphase solutions; in other words, the coupling and delay parameters can be chosen so that the two modes of behavior are both stable, a phenomenon of bi-rhythmicity.

APPLICATIONS TO SCENE ANALYSIS

A natural scene generally contains multiple objects, each of which can be viewed as a group of similar sensory features. A major motivation behind studies on oscillatory correlation is scene analysis, or the segmentation of a scene into a set of coherent objects. Scene segmentation, or perceptual organization, plays a critical role in the understanding of natural scenes. Although humans perform it with apparent ease, the general problem of scene segmentation remains unsolved in sensory and perceptual information processing.

Oscillatory correlation provides an elegant and unique way to represent results of segmentation. As illustrated in Fig. 7, segmentation is performed in *time*; after segmentation, each segment pops out at a distinct time from the network and different segments alternate in time. On the basis of synchronization and desynchronization properties in relaxation oscillator networks, substantial progress has been made to address the scene segmentation problem; see Wang [26] for a comprehensive review.

Image Segmentation

Wang and Terman [22] studied LEGION for segmenting real images. In order to perform effective segmentation, LEGION needs to be extended to handle images with noisy regions. Without such extension, LEGION would treat each region, no matter how small it is, as a separate segment, resulting in many fragments. A large number of fragments degrade segmentation results, and a more serious problem is that it is difficult for LEGION to produce more than several (5 to 10) segments. In general, with a fixed set of parameters, LEGION can segment only a limited number of patterns [11]. This number depends on the ratio of the times that a single oscillator spends in the silent and active phases; see, for example, Figs. 3 and 7. This limit is called the *segmentation capacity* of LEGION [22]. Noisy fragments therefore compete with major image regions for becoming segments, and the major segments may not be extracted as a result. To address this problem of fragmentation, they introduced the notion of lateral potential for each oscillator, which allows the network to distinguish between major blocks and noisy fragments. The basic idea is that a major block must contain at least one oscillator, denoted as a leader, which lies in the center area of a large homogeneous image region. Such an oscillator receives large lateral excitation from its neighborhood, and thus its lateral potential is charged high. A noisy fragment does not contain such an oscillator.

More specifically, a new variable p_i denoting the lateral potential for each oscillator i is introduced into the definition of the oscillator (cf. (6)). $p_i \to 1$ if i frequently receives a high weighted sum from its neighborhood, signifying that i is a leader, and the value of p_i determines whether or not the oscillator i is a leader. After an initial time period, only leaders can jump up without lateral excitation from other oscillators. When a leader jumps up, it spreads its activity to other oscillators within its own block, so they can also jump up. Oscillators not in this block are prevented from jumping up because of the global inhibitor. Without a leader, the oscillators corresponding to noisy fragments cannot jump up beyond the initial period. The collection of all noisy regions is called the *background*, which is generally discontiguous.

Wang and Terman obtained a number of rigorous results concerning the extended version of LEGION [22]. The main analytical result states that the oscillators with low lateral potentials will become excitable after a beginning period, and the asymptotic behavior of each oscillator belonging to a major region is precisely the same as the network obtained by simply removing all noisy regions. Given the Terman-Wang theorem on original LEGION, this implies that after a number of cycles a block of oscillators corresponding to a major region synchronizes, while any two blocks corresponding to different major regions desynchronize. Also, the number of periods required for segmentation is no greater than the number of major regions plus one.

For gray-level images, each oscillator corresponds to a pixel. In a simple scheme for setting up lateral connections, two neighboring oscillators are connected with a weight proportional to corresponding pixel similarity. To illustrate typical segmentation results, Fig. 9(a) displays a gray-level aerial image to be segmented. To speed up simulation with a large number of oscillators needed for processing real images, Wang and Terman abstracted an algorithm that follows LEGION dynamics [22]. Fig. 9(b) shows the result of segmentation by the algorithm. The entire image is segmented into 23 regions, each of which corresponds to a different intensity level in the figure, which indicates the phases of oscillators. In the simulation, different segments rapidly popped out from the image, as similarly shown in Fig. 7. As can be seen from Fig. 9(b), most of the major regions were segmented, including the central lake, major parkways, and various fields. The black scattered regions in the figure represent the background that remains inactive. Due to the use of lateral potentials, all these tiny regions stay in the background.

Auditory Scene Analysis

A listener in an auditory environment is generally exposed to acoustic energy from different sources. In order to understand the auditory environment, the listener must first disentangle the acoustic wave reaching the ears. This process is referred to as *auditory scene analysis*. According to Bregman [27], auditory scene analysis takes place in two stages. In the first stage, the acoustic mixture reaching the ears is decomposed into a collection of sensory elements (or segments). In the second stage, segments that likely arise from the same source are grouped to form a stream that is

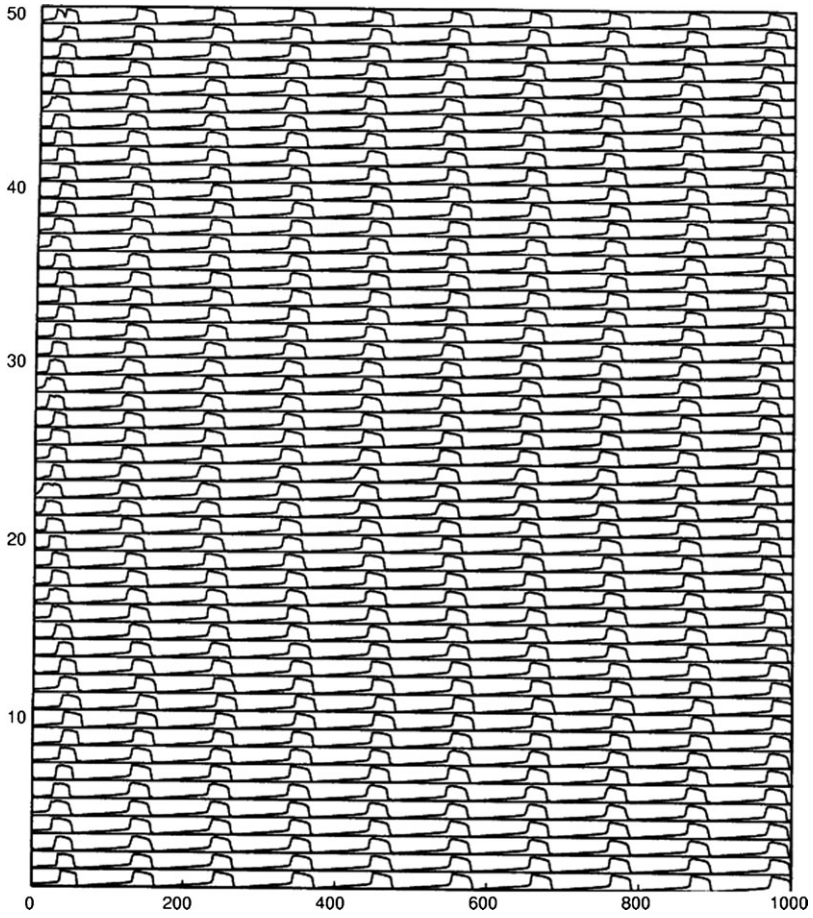

Figure 8. Loose synchrony in a chain of 50 relaxation oscillators (from [23]). This network achieves loose synchrony and stability by the third period of oscillation.

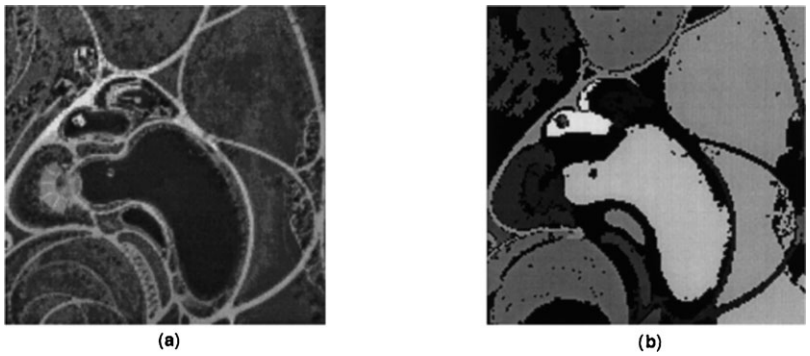

Figure 9. Image segmentation (from [22]). (a) A gray-level image consisting of 160 × 160 pixels. (b) Result of segmenting the image in (a). Each segment is indicated by a distinct gray level. The system produces 23 segments plus a background, which is indicated by the black scattered regions in the figure.

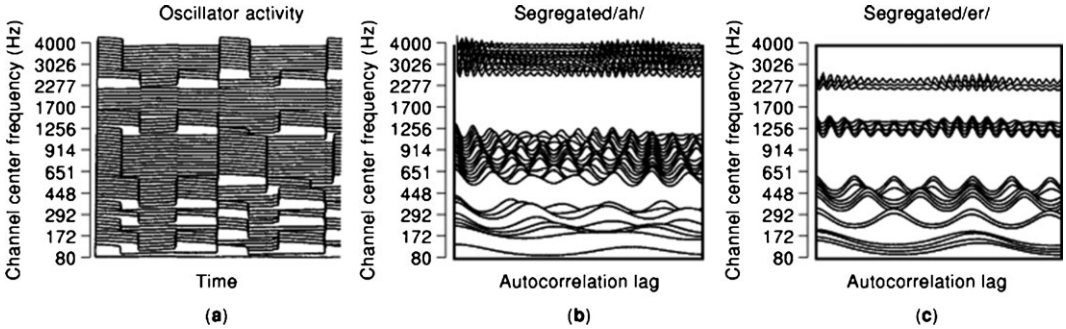

Figure 10. Speech segregation (from [30]). (a) Peripheral responses to a mixture of voiced utterance and telephone ringing. The 2-D response is produced by 128 auditory filters with center frequencies ranging from 80 Hz to 5 kHz, over 150 time frames. (b) Segregated speech that is indicated by white pixels representing active oscillators at a time. (c) Segregated background that is indicated by white pixels representing active oscillators at a different time.

a perceptual representation of an auditory event.

Auditory segregation was first studied from the oscillatory correlation perspective by von der Malsburg and Schneider [14]. They constructed a fully connected oscillator network, each oscillator representing a specific auditory feature. Additionally, there is a global inhibitory oscillator introduced to segregate oscillator groups. With a mechanism of rapid modulation of connection strengths, they simulated segregation based on onset synchrony, i.e., oscillators simultaneously triggered synchronize with each other, and these oscillators desynchronize with those representing another stream presented at a different time. However, due to global connectivity that is unable to encode topological relations, their model cannot simulate the basic phenomenon of stream segregation.

By extending LEGION to the auditory domain, Wang proposed an oscillator network for addressing stream segregation [28]. The basic architecture is a 2-D LEGION network, where one dimension represents time and another represents frequency. This network, plus systematic delay lines, can group auditory features into a stream by phase synchronization and segregate different streams by desynchronization. The network demonstrates a set of psychological phenomena regarding auditory scene analysis, including dependency on frequency proximity and temporal proximity, sequential capturing, and competition among different perceptual organizations [27]. Brown and Wang [29] used an array of relaxation oscillators for modeling the perceptual segregation of double vowels. It is well documented that the ability of listeners to identify two simultaneously presented vowels is improved by introducing a difference in fundamental frequency (F0) between the vowels. Prior to the oscillator array, an auditory mixture is processed by an auditory filterbank, which decompose an acoustic signal into a number of frequency channels. Each oscillator in the array receives an excitatory input from its corresponding frequency channel. In addition, each oscillator sends excitation to a global inhibitor which in turn feeds back inhibition. The global inhibitor ensures that weakly correlated groups of oscillators desynchronize to form different streams. Simulations on a vowel set used in psychophysical studies confirm that the results produced by their oscillator array qualitatively match the performance of human listeners; in particular vowel identification performance increases with increasing difference in F0.

Subsequently, Wang and Brown [30] studied a more difficult problem, speech segregation, on the basis of oscillatory correlation. Their model embodies Bregman's two-stage conceptual model by introducing a two-layer network of relaxation oscillators. The first layer is a LEGION network with time and frequency axes that segments an auditory input into a collection of contiguous time-frequency regions. This segmentation is based on cross-channel correlation between adjacent frequency channels and temporal continuity. The second layer, which is a laterally connected network, then groups auditory segments produced in the first layer on the basis of common periodicity. More specifically, dominant F0 detected within a time frame is used to divide all frequency channels into those that are consistent with F0 and the rest. As a result, the second layer segregates the segments into a foreground stream and the background. Figure 10 shows an example of segregating a mixture of a voiced utterance and telephone ringing. The input mixture after peripheral analysis is displayed in Fig. 10(a). The segregated speech stream and the background are shown in Figs. 10(b) and 10(c), respectively, where a segment corresponds to a connected region.

CONCLUDING REMARKS

Relaxation oscillations are characterized by two time scales, and exhibit qualitatively different behaviors than sinusoidal or harmonic oscillations. This distinction is particularly prominent in synchronization and desynchronization in networks of relaxation oscillators. The unique properties in relaxation oscillators have led to new and promising applications to neural computation, including scene analysis. It should be noted that networks of relaxation oscillations often lead to very complex behaviors other than synchronous and antiphase solutions. Even with identical oscillators and nearest neighbor coupling, traveling waves and other complex spatiotemporal patterns can occur [31].

Relaxation oscillations with a singular parameter lend themselves to analysis by singular perturbation theory [32]. Singular perturbation theory in turn yields a geometric approach to analyzing relaxation oscillation systems, as illustrated in Figs. 4 and 6. Also based on singular solutions, Linsay and Wang [33] proposed a fast method to numerically integrate relaxation oscillator networks. Their technique, called the singular limit method, is derived in the singular limit $\varepsilon \to 0$. A numerical algorithm is given for the LEGION network, and it produces large speedup compared to commonly used integration methods such as the Runge-Kutta method. The singular limit method makes it possible to simulate large-scale networks of relaxation oscillators.

Computation using relaxation oscillator networks is inherently parallel, where each single oscillator operates in parallel with all the other oscillators. This feature, plus continuous-time dynamics makes oscillator networks attractive for direct hardware implementation. Using CMOS technology, for example, Cosp and Madrenas [34] fabricated a VLSI chip for a 16×16 LEGION network and used the chip for a number of segmentation tasks. With its dynamical and biological foundations, oscillatory correlation promise to offer a general computational framework.

ACKNOWLEDGMENTS

The preparation for this article was supported in part by an AFOSR grant (FA9550-04-1-0117) and an NSF grant (IIS-0534707).

BIBLIOGRAPHY

1. B. van der Pol," On 'relaxation oscillations'," *Philosophical Magazine*, vol.**2**,pp. 978–992, 1926.
2. B. van der Pol," Biological rhythms considered as relaxation oscillations," *Acta Med. Scand. Suppl.*, vol.**108**,pp. 76–87, 1940.

3. A. V. Hill," Wave transmission as the basis of nerve activity," *Cold Spring Harbour Symp. on Quant. Biol.*, vol.**1**,pp. 146–151, 1933.
4. J. Grassman, *Asymptotic methods for relaxation oscillations and applications*. New York: Springer-Verlag, 1987.
5. A. L. Hodgkin and A. F. Huxley," A quantitative description of membrane current and its application to conduction and excitation in nerve," *J. Physiol. (Lond.)*, vol.**117**,pp. 500–544, 1952.
6. J. P. Keener," Analog circuitry for the van der Pol and FitzHugh-Nagumo equations," *IEEE Trans. Syst. Man Cybern.*, vol.**13**,pp. 1010–1014, 1983.
7. R. FitzHugh," Impulses and physiological states in models of nerve membrane," *Biophys. J.*, vol.**1**,pp. 445–466, 1961.
8. J. Nagumo, S. Arimoto, and S. Yoshizawa," An active pulse transmission line simulating nerve axon," *Proc. IRE*, vol.**50**,pp. 2061–2070, 1962.
9. C. Morris and H. Lecar," Voltage oscillations in the barnacle giant muscle fiber," *Biophys. J.*, vol.**35**,pp. 193–213, 1981.
10. J. Rinzel and G. B. Ermentrout," Analysis of neural excitability and oscillations," in *Methods in neuroal modeling*, C. Koch andI. Segev, Eds. Cambridge MA: MIT Press, 1989, pp. 135–169.
11. D. Terman and D. L. Wang," Global competition and local cooperation in a network of neural oscillators," *Physica D*, vol.**81**,pp. 148–176, 1995.
12. R. Eckhorn, R. Bauer, W. Jordan, M. Brosch, W. Kruse, M. Munk, and H. J. Reitboeck," Coherent oscillations: A mechanism of feature linking in the visual cortex," *Biol. Cybern.*, vol.**60**,pp. 121–130, 1988.
13. C. M. Gray, P. König, A. K. Engel, and W. Singer," Oscillatory responses in cat visual cortex exhibit inter-columnar synchronization which reflects global stimulus properties," *Nature*, vol.**338**,pp. 334–337, 1989.
14. C. von der Malsburg and W. Schneider," A neural cocktail-party processor," *Biol. Cybern.*, vol.**54**,pp. 29–40, 1986.
15. N. D. Mermin and H. Wagner," Absence of ferromagnetism or antiferromagnetism in one- or two-dimensional isotropic Heisenberg models," *Phys. Rev. Lett.*, vol.**17**,pp. 1133–1136, 1966.
16. D. Somers and N. Kopell," Rapid synchrony through fast threshold modulation," *Biol. Cybern.*, vol.**68**,pp. 393–407, 1993.
17. D. L. Wang," Modeling global synchrony in the visual cortex by locally coupled neural oscillators,"In *Proc. of 15th Ann. Conf. Cognit. Sci. Soc.*,Boulder CO, 1993.
18. H. R. Wilson and J. D. Cowan," Excitatory and inhibitory interactions in localized populations of model neurons," *Biophys. J.*, vol.**12**,pp. 1–24, 1972.
19. S. R. Campbell, D. L. Wang, and C. Jayaprakash," Synchronization rates in classes of relaxation oscillators," *IEEE Trans. Neural Net.*, vol.**15**,pp. 1027–1038, 2004.
20. D. L. Wang and D. Terman," Locally excitatory globally inhibitory oscillator networks," *IEEE Trans. Neural Net.*, vol.**6**,pp. 283–286, 1995.
21. D. L. Wang," Emergent synchrony in locally coupled neural oscillators," *IEEE Trans. Neural Net.*, vol.**6**,pp. 941–948, 1995.
22. D. L. Wang and D. Terman," Image segmentation based on oscillatory correlation," *Neural Comp.*, vol.**9**,pp. 805–836(for errata see *Neural Comp.*, vol.**9**,pp. 1623–1626, 1997), 1997.
23. S. R. Campbell and D. L. Wang," Relaxation oscillators with time delay coupling," *Physica D*, vol.**111**,pp. 151–178, 1998.
24. J. J. Fox, C. Jayaprakash, D. L. Wang, and S. R. Campbell," Synchronization in relaxation oscillator networks with conduction delays," *Neural Comp.*, vol.**13**,pp. 1003–1021, 2001.
25. A. K. Sen and R. H. Rand," A numerical investigation of the dynamics of a system of two time-delay coupled relaxation oscillators," *Comm. Pure Appl. Anal.*, vol.**2**,pp. 567–577, 2003.
26. D. L. Wang," The time dimension for scene analysis," *IEEE Trans. Neural Net.*, vol.**16**,pp. 1401–1426, 2005.
27. A. S. Bregman, *Auditory scene analysis*. Cambridge MA: MIT Press, 1990.
28. D. L. Wang," Primitive auditory segregation based on oscillatory correlation," *Cognit. Sci.*, vol.**20**,pp. 409–456, 1996.
29. G. J. Brown and D. L. Wang," Modelling the perceptual segregation of double vowels with a network of neural oscillators," *Neural Net.*, vol.**10**,pp. 1547–1558, 1997.
30. D. L. Wang and G. J. Brown," Separation of speech from interfering sounds based on oscillatory correlation," *IEEE Trans. Neural Net.*, vol.**10**,pp. 684–697, 1999.
31. S. Campbell," *Synchrony and desynchrony in neural oscillators*,"Ph.D. Dissertation, The Ohio State University Department of Physics, 1997.
32. N. Fenichel," Geometrical singular perturbation theory for ordinary differential equations," *J. Diff. Eq.*, vol.**31**,pp. 53–98, 1979.
33. P. S. Linsay and D. L. Wang," Fast numerical integration of relaxation oscillator networks based on singular limit solutions," *IEEE Trans. Neural Net.*, vol.**9**,pp. 523–532, 1998.
34. J. Cosp and J. Madrenas," Scene segmentation using neuromorphic oscillatory networks," *IEEE Trans. Neural Net.*, vol.**14**,pp. 1278–1296, 2003.

DELIANG WANG
Department of Computer
Science & Engineering
Center for Cognitive Science,
The Ohio State University,
Columbus, OH, 43210-1277